Academic Journal of Science and Technology
ISSN: 2771-3032 | Vol. 14, No. 3, 2025

Application of Square-Root Information Kalman Filtering to Combined Navigation Systems

Yifan Yang, Yanmin Luo

Xi 'an Shiyou University, Xi 'an 710065, China

Abstract: With the rapid development of modern science and technology, navigation technology plays a crucial role in transportation, aerospace, military and other fields. At present, a single navigation technology has been difficult to meet the complex navigation needs of high mobility carriers or special environments. Aiming at the above problems, this paper carries out an in-depth study on the tightly coupled navigation system of Strapdown Inertial Navigation System (SINS) and Global Navigation Satellite System (GNSS), and introduces the square-root information Kalman filtering algorithm. The algorithm takes the information matrix (the inverse of the mean square error matrix) as the updating object, which effectively avoids the numerical instability and non-positive characterization problems that may occur in the iterative process of the mean square error matrix. Compared with the traditional extended Kalman filter, the square-root information Kalman filter has higher numerical stability and computational efficiency in dealing with nonlinear systems, which is especially suitable for multi-sensor fusion scenarios.

Keywords: Inertial navigation; Tight coupling navigation; Extended Kalman filter; Square-root information Kalman filtering.

1. Introduction

With the rapid development of modern navigation technology, the demand for high-precision and high-reliability navigation and localization is growing in military, civil and industrial fields. In complex environments such as urban canyons, tunnels, underground spaces or electromagnetic interference scenarios, it is often difficult for a single navigation system to meet the actual needs. For example, global navigation satellite systems rely on external signals and are susceptible to occlusion or interference, while inertial navigation systems, though autonomous, accumulate errors over time[1]. Combining the Strapdown Inertial Navigation System with the global navigation satellite systems can combine the advantages of inertial navigation's strong anti-jamming ability and the advantages of satellite navigation's high long-term accuracy to form a complementary system.

There are three main combinations of current combined inertial/satellite navigation systems, namely loose coupling[2], tight coupling[3] and deep coupling[4]. The loose combination approach simply fuses the outputs of an inertial navigation system and a satellite navigation system, usually by correcting the errors of the inertial navigation system through a Kalman filter. In the tight coupling approach, the pseudorange and Doppler shift of the satellite navigation system are directly fused with the state quantities of the inertial navigation system, enabling better utilization of satellite navigation information. The deep combination approach, on the other hand, deeply integrates the receiver of the satellite navigation system with the inertial navigation system, and even fuses them at the signal processing level to further improve the system's anti-interference capability and reliability.

Kalman filtering is the core algorithm for state estimation, the traditional Kalman filtering algorithm assumes that the system is linear and the noise is Gaussian distribution, in order to the nonlinear system model and non-Gaussian noise, the researchers proposed the extended Kalman filtering algorithm, which linearizes the nonlinear model through the Taylor Expansion[5], but it is prone to dispersion in the strong nonlinear scenario. Some scholars have proposed several adaptive algorithms, such as the Sage-Husa algorithm, which can dynamically adjust the noise covariance matrix R to improve the robustness to abrupt noise, and is suitable for intermittent satellite signal scenarios. Aiming at the limitations of the EKF algorithm, based on the filtering method of nonlinear transformation, the vast number of scholars have also proposed the traceless Kalman filter and the volumetric Kalman filter. UKF approximates the nonlinear distribution through the traceless transformation, avoids the calculation of Jacobi matrix, and improves the positioning accuracy by about 20% compared with the EKF in the inertial/satellite tight coupling.

In recent years, deep learning has been used to combine with traditional Kalman filtering algorithms to produce neural network-assisted Kalman filtering methods, which utilize LSTM networks to predict inertial device errors, and end-to-end filtering networks that directly model the observation of noise characteristics through CNN-Transformer networks, which can replace the manual noise modeling of traditional Kalman filtering, and show stronger Adaptability in dynamic interference scenarios. Aiming at the problem that the mean square error matrix in Kalman filtering tends to lose its positive definiteness and the demand of multi-sensor fusion, square-root filtering and information filtering are proposed in this paper. Square-root filtering updates the square-root of the mean square error matrix by Cholesky decomposition or QR decomposition to improve numerical stability. Information filtering takes the information matrix, which is the inverse of the mean square error matrix, as the updating object to avoid matrix inversion, making it more suitable for multi-sensor data fusion.

2. SINS/GNSS Tightly Coupled Navigation System

In the tight coupling system, the global satellite receiver provides the raw information pseudorange and pseudorange rate used for localization to the Kalman filter, and the errors of each pseudorange and pseudorange rate are independent of each other. The strapdown inertial navigation system (SINS) solution module receives the specific force and angular rate information output from the IMU, generates the navigation output position and velocity information for the SINS, and calculates the pseudorange and pseudorange rate by combining this information with the ephemeris generated by the satellite receiver. The differences in pseudorange and pseudorange rate between those derived from the strapdown inertial navigation system (SINS) information and those generated by the satellite receiver are used as inputs to the Kalman filter to obtain the state error estimate of the SINS.

The gyro drift and accelerometer bias in this state error estimate are fed back to the strapdown inertial navigation system (SINS) for correction. The position and velocity errors in the SINS, after being corrected using the position and velocity errors from this state error estimate, are then used as the final results of the tightly coupled SINS/GNSS navigation system[6]. The architecture of the tightly coupled system is shown in Figure 1.

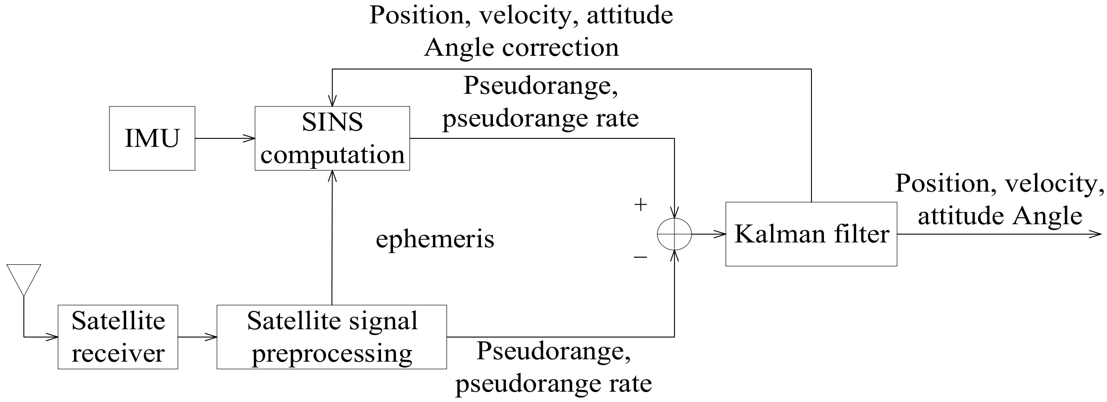

Figure 1. The architecture of SINS/GNSS tightly coupled system

(1) SINS/GNSS error update equation

The SINS error state consists of the position error $\boldsymbol{\delta p}$, the velocity error $\boldsymbol{\delta v^n}$, the attitude error Angle $\boldsymbol{\varphi^n}$, the gyroscope error $\boldsymbol{\varepsilon^b}$ and the accelerometer error $\boldsymbol{\nabla^b}$.

The error state vector[7] is

$\boldsymbol{X_I} = [\delta L\ \ \delta\lambda\ \ \delta h\ \ \delta v_x\ \ \delta v_y\ \ \delta v_z\ \ \varphi_x\ \ \varphi_y\ \ \varphi_z\ \ \varepsilon_{bx}\ \ \varepsilon_{by}\ \ \varepsilon_{bz}\ \ \nabla_{bx}\ \ \nabla_{by}\ \ \nabla_{bz}]^{\mathrm{T}}$.

In the equation, δL is the latitude error, $\delta\lambda$ is the longitude error, δh is the altitude error. The b-frame is the body frame, and the n-frame is the navigation frame.

The error state equation of the SINS is expressed as:

$$\dot{\boldsymbol{X}}_{\boldsymbol{I}} = \boldsymbol{F_I X_I} + \boldsymbol{G_I W_I} \tag{1}$$

In the equation, the system noise $\boldsymbol{W_I} = \left[w_{gx}\ w_{gy}\ w_{gz}\ w_{ax}\ w_{ay}\ w_{az}\right]^{\mathrm{T}}$, represents the components of the gyroscope angular velocity measurement noise and the accelerometer specific force measurement noise in the three coordinate directions of the b-frame[8]. $\boldsymbol{F_I}$ is the inertial navigation state matrix, and $\boldsymbol{G_I}$ is the inertial navigation noise matrix.

The main errors in satellite navigation systems are clock bias and clock drift. Equivalent range errors and velocity errors are selected as the error states of the satellites in the tightly coupled system.The GNSS error state equation is expressed as:

$$\dot{\delta t}_{\mathrm{u}} = \delta t_{\mathrm{ru}} + w_{\mathrm{tu}} \tag{2}$$

$$\dot{\delta t}_{\mathrm{ru}} = w_{\mathrm{tru}} \tag{3}$$

In the equation, δt_{u} and δt_{ru} represent the range and range rate corresponding to the receiver clock bias and clock drift, respectively[9]. w_{tu} and w_{tru} are white nois. The equation can be represented in matrix form as:

$$\dot{\boldsymbol{X}}_{\boldsymbol{B}} = \boldsymbol{F_B X_B} + \boldsymbol{G_B W_B} \tag{4}$$

In the equation, $\boldsymbol{X_B} = [\delta t_{\mathrm{u}}\ \ \delta t_{\mathrm{ru}}]^{\mathrm{T}}$, $\boldsymbol{W_B} = [w_{\mathrm{tu}}\quad w_{\mathrm{tru}}]^{\mathrm{T}}$.

By combining the SINS error state equation (1) with the GNSS error state equation (4), the tightly coupled navigation system state equation can be obtained[10]:

$$\begin{bmatrix} \dot{\boldsymbol{X}}_{\boldsymbol{I}} \\ \dot{\boldsymbol{X}}_{\boldsymbol{B}} \end{bmatrix} = \begin{bmatrix} \boldsymbol{F_I} & \boldsymbol{O} \\ \boldsymbol{O} & \boldsymbol{F_B} \end{bmatrix} \begin{bmatrix} \boldsymbol{X_I} \\ \boldsymbol{X_B} \end{bmatrix} + \begin{bmatrix} \boldsymbol{G_I} & \boldsymbol{O} \\ \boldsymbol{O} & \boldsymbol{G_B} \end{bmatrix} \begin{bmatrix} \boldsymbol{W_I} \\ \boldsymbol{W_B} \end{bmatrix} \tag{5}$$

That is:

$$\dot{\boldsymbol{X}}_{\boldsymbol{t}} = \boldsymbol{F_t X_t} + \boldsymbol{G_t W_t} \tag{6}$$

(2) System Measurement Equation

In the tightly coupled navigation system, the measurement information mainly consists of the differences in pseudorange and pseudorange rate. Specifically, the system employs the differences between the pseudoranges and pseudorange rates calculated by the SINS and those measured by the GNSS as the measurement information[11]. This measurement approach enables the direct utilization of raw GNSS observations, thereby facilitating more precise error modeling and higher navigation accuracy. The measurement equation of the tightly coupled system is given by:

$$\boldsymbol{Z_t} = \begin{bmatrix} \boldsymbol{H_\rho} \\ \boldsymbol{H_{\dot\rho}} \end{bmatrix} \boldsymbol{X_t} + \begin{bmatrix} \boldsymbol{V_\rho} \\ \boldsymbol{V_{\dot\rho}} \end{bmatrix} = \boldsymbol{H_t X_t} + \boldsymbol{V_t} \tag{7}$$

The pseudorange and pseudorange rate measurement equations play a significant role in the tightly coupled inertial and satellite navigation system. By integrating data from the inertial navigation system, they notably enhance navigation accuracy and reliability.

3. Extended Kalman Filter

The core idea of the Extended Kalman Filter (EKF) is to linearize the nonlinear system through a Taylor series expansion, ignoring higher-order terms. In this paper, the Taylor series is expanded to the first order. Assume the discrete-time state-space nonlinear model is given by:

$$\begin{cases} \boldsymbol{X_k} = \boldsymbol{f}(\boldsymbol{X_{k-1}}) + \boldsymbol{\Gamma_{k-1}} \boldsymbol{W_{k-1}} \\ \boldsymbol{Z_k} = \boldsymbol{h}(\boldsymbol{X_k}) + \boldsymbol{V_k} \end{cases} \tag{8}$$

In the equations, $\begin{cases} E[\boldsymbol{W_k}] = 0, \ E\left[\boldsymbol{W_k W_j^{\mathrm{T}}}\right] = \boldsymbol{Q_k} \delta_{kj} \\ E[\boldsymbol{V_k}] = 0, \ E\left[\boldsymbol{V_k V_k^{\mathrm{T}}}\right] = \boldsymbol{R_k} \delta_{kj} \\ E\left[\boldsymbol{W_k V_j^{\mathrm{T}}}\right] = 0 \end{cases}$, where $\boldsymbol{X_k}$ is the n-dimensional state vector, $\boldsymbol{f}(\boldsymbol{X_k}) = [f_1(\boldsymbol{X_k}) \ f_2(\boldsymbol{X_k}) \ \ldots f_n(\boldsymbol{X_k})]^{\mathrm{T}}$ is the n-dimensional nonlinear vector function, $\boldsymbol{Z_k}$ is the m-dimensional measurement vector, $\boldsymbol{h}(\boldsymbol{X_k}) = [h_1(\boldsymbol{X_k}) \ h_2(\boldsymbol{X_k}) \ \ldots h_m(\boldsymbol{X_k})]^{\mathrm{T}}$ is the m-dimensional nonlinear vector function, $\boldsymbol{\Gamma_{k-1}}$ is the system noise distribution matrix, $\boldsymbol{W_{k-1}}$ is the system noise vector, and $\boldsymbol{V_k}$ is the m-dimensional measurement noise vector.

The EKF filtering equations for the nonlinear system with state X_k are given by[12]:

$$\begin{cases} \boldsymbol{\hat{X}_{k/k-1}} = \boldsymbol{f}(\boldsymbol{\hat{X}_{k-1}}) \\ \boldsymbol{P_{k/k-1}} = \boldsymbol{\Phi_{k/k-1}} \boldsymbol{P_{k-1}} \boldsymbol{\Phi_{k/k-1}^{\mathrm{T}}} + \boldsymbol{\Gamma_{k-1}} \boldsymbol{Q_{k-1}} \boldsymbol{\Gamma_{k-1}^{\mathrm{T}}} \\ \boldsymbol{K_k} = \boldsymbol{P_{k/k-1}} \boldsymbol{H_k^{\mathrm{T}}} (\boldsymbol{H_k} \boldsymbol{P_{k/k-1}} \boldsymbol{H_k^{\mathrm{T}}} + \boldsymbol{R_k})^{-1} \\ \boldsymbol{\hat{X}_k} = \boldsymbol{\hat{X}_{k/k-1}} + \boldsymbol{K_k} [\boldsymbol{Z_k} - \boldsymbol{h}(\boldsymbol{\hat{X}_{k/k-1}})] \\ \boldsymbol{P_k} = (\boldsymbol{I} - \boldsymbol{K_k} \boldsymbol{H_k}) \boldsymbol{P_{k/k-1}} \end{cases} \tag{9}$$

In the equations, $\boldsymbol{\Phi_{k/k-1}}$ is the system Jacobian matrix, $\boldsymbol{\Phi_{k/k-1}} = \boldsymbol{J}(\boldsymbol{f}(\boldsymbol{\hat{X}_{k-1}}))$, and $\boldsymbol{H_k}$ is the measurement Jacobian matrix, $\boldsymbol{H_k} = \boldsymbol{J}(\boldsymbol{h}(\boldsymbol{\hat{X}_{k/k-1}}))$. If the nonlinear functions are complex to differentiate or even non-differentiable, the first-order partial derivatives can be approximated using the central difference method.

4. Square-Root Information Kalman Filter Algorithm

(1) Potter Square-Root Filtering

The Potter square-root filtering decomposes the mean square error matrix P into the product of a lower triangular matrix Δ , that is, $P = \Delta\Delta^T$, and operates solely on these lower triangular matrices during the filtering process. This approach reduces numerical errors caused by the ill-conditioning of the mean square error matrix.

Assume the square-roots of the mean square error matrices $\boldsymbol{P_{k-1}}$, $\boldsymbol{P_{k/(k-1)}}$, and $\boldsymbol{P_k}$ are $\Delta_{\boldsymbol{k-1}}$, $\Delta_{\boldsymbol{k/(k-1)}}$, and $\Delta_{\boldsymbol{k}}$, respectively. The measurement update of the state estimation mean square error matrix and its corresponding square-root filtering equations are given by:

$$\boldsymbol{P_k} = \boldsymbol{P_{k/(k-1)}} - \boldsymbol{P_{k/(k-1)}} \boldsymbol{H_k^{\mathrm{T}}} (\boldsymbol{H_k} \boldsymbol{P_{k/(k-1)}} \boldsymbol{H_k^{\mathrm{T}}} + \boldsymbol{R_k})^{-1} \boldsymbol{H_k} \boldsymbol{P_{k/(k-1)}} \tag{10}$$

$$\boldsymbol{\Delta_k} = \boldsymbol{\Delta_{k/(k-1)}} [\boldsymbol{I} - \boldsymbol{\Delta_{k/(k-1)}^{\mathrm{T}}} \boldsymbol{H_k^{\mathrm{T}}} (\boldsymbol{\rho_k} \boldsymbol{\rho_k^{\mathrm{T}}} + \boldsymbol{R_k^{\frac{1}{2}}} \boldsymbol{\rho_k^{\mathrm{T}}})^{-1} \boldsymbol{H_k} \boldsymbol{\Delta_{k/(k-1)}}] \tag{11}$$

In the equations, $\boldsymbol{R_k^{\frac{1}{2}}}$ denotes the square-root matrix of $\boldsymbol{R_k}$. The matrix $\boldsymbol{\rho_k}$ satisfies $\boldsymbol{\rho_k \rho_k^{\mathrm{T}}} = \boldsymbol{H_k P_{k/(k-1)} H_k^{\mathrm{T}}} + \boldsymbol{R_k} = \begin{bmatrix} \boldsymbol{H_k \Delta_{k/(k-1)}} & \boldsymbol{R_k^{\frac{1}{2}}} \end{bmatrix} \begin{bmatrix} \boldsymbol{\Delta_{k/(k-1)}^{\mathrm{T}} H_k^{\mathrm{T}}} \\ (\boldsymbol{R_k^{\frac{1}{2}}})^{\mathrm{T}} \end{bmatrix}$. The square-root matrix ρ_k is obtained using the QR decomposition method.

(2) Information Filtering and Information Fusion

The information matrix is the inverse of the mean square error matrix[13], while the information vector is the product of the state estimate and the information matrix. This representation makes information filtering more efficient and intuitive when dealing with multi-sensor data fusion and distributed systems. Let $\mathbb{I}_{\boldsymbol{k}} = \boldsymbol{P_k^{-1}}$ [14]. Then, the so-called information filtering equations expressed in terms of the information matrix are given by:

$$\begin{cases} \mathbb{I}_{\boldsymbol{k/(k-1)}} = (\boldsymbol{\Phi_{k/(k-1)}} \mathbb{I}_{\boldsymbol{k-1}}^{-1} \boldsymbol{\Phi_{k/(k-1)}^{\mathrm{T}}} + \boldsymbol{\Gamma_{k-1}} \boldsymbol{Q_{k-1}} \boldsymbol{\Gamma_{k-1}^{\mathrm{T}}})^{-1} \\ \mathbb{I}_{\boldsymbol{k}} = \mathbb{I}_{\boldsymbol{k/(k-1)}} + \boldsymbol{H_k^{\mathrm{T}}} \boldsymbol{R_k^{-1}} \boldsymbol{H_k} \\ \boldsymbol{K_k} = \mathbb{I}_{\boldsymbol{k}}^{-1} \boldsymbol{H_k^{\mathrm{T}}} \boldsymbol{R_k^{-1}} \\ \boldsymbol{\hat{X}_{k/(k-1)}} = \boldsymbol{\Phi_{k/(k-1)}} \boldsymbol{\hat{X}_{k-1}} \\ \boldsymbol{\hat{X}_k} = \boldsymbol{\hat{X}_{k/(k-1)}} + \boldsymbol{K_k} (\boldsymbol{Z_k} - \boldsymbol{H_k} \boldsymbol{\hat{X}_{k/(k-1)}}) \end{cases} \tag{12}$$

(3) Square-Root Information Extended Kalman Filter

Let the square-roots of the information matrices $\mathbb{I}_{\boldsymbol{k}}$ and $\mathbb{I}_{\boldsymbol{k/(k-1)}}$ be denoted as $\mathbb{I}_{\boldsymbol{k}} = \boldsymbol{\xi_k \xi_k^{\mathrm{T}}}$ and $\mathbb{I}_{\boldsymbol{k/(k-1)}} = \boldsymbol{\xi_{k/(k-1)} \xi_{k/(k-1)}^{\mathrm{T}}}$, respectively.

The information prediction equation is given by:

$$\mathbb{I}_{\boldsymbol{k/(k-1)}} = \boldsymbol{\Phi_{k/(k-1)}^{-\mathrm{T}}} \mathbb{I}_{\boldsymbol{k-1}} \boldsymbol{\Phi_{k/(k-1)}^{-1}} - \boldsymbol{\Phi_{k/(k-1)}^{-\mathrm{T}}} \mathbb{I}_{\boldsymbol{k-1}} \boldsymbol{\Phi_{k/(k-1)}^{-1}} \boldsymbol{\Gamma_{k-1}} (\boldsymbol{\Gamma_{k-1}^{\mathrm{T}}} \boldsymbol{\Phi_{k/(k-1)}^{-\mathrm{T}}} \mathbb{I}_{\boldsymbol{k-1}} \boldsymbol{\Phi_{k/(k-1)}^{-1}} \boldsymbol{\Gamma_{k-1}} + \boldsymbol{Q_{k-1}^{-1}})^{-1} \times \boldsymbol{\Gamma_{k-1}^{\mathrm{T}}} \boldsymbol{\Phi_{k/(k-1)}^{-\mathrm{T}}} \mathbb{I}_{\boldsymbol{k-1}} \boldsymbol{\Phi_{k/(k-1)}^{-1}} \tag{13}$$

Analogous to the mean square error matrix update in the standard Kalman filter, the square-root information Kalman filter time update algorithm can be obtained by replacing the symbols $\boldsymbol{\Delta_k} \to \boldsymbol{\xi_{k/(k-1)}}$, $\boldsymbol{\Delta_{k/(k-1)}} \to \boldsymbol{\Phi^{-\mathrm{T}}_{k/(k-1)}\xi_{k-1}}$, $\boldsymbol{H_k} \to \boldsymbol{\Gamma^{\mathrm{T}}_{k-1}}$及$\boldsymbol{R_k^{\frac{1}{2}}} \to (\boldsymbol{Q_{k-1}^{-\frac{1}{2}}})^{\mathrm{T}}$.

$$\boldsymbol{\xi_{k/(k-1)}} = \boldsymbol{\Phi^{-\mathrm{T}}_{k/(k-1)}\xi_{k-1}}\left\{\boldsymbol{I} - \boldsymbol{\xi^{\mathrm{T}}_{k-1}\Phi^{-1}_{k/(k-1)}\Gamma_{k-1}}\left[\boldsymbol{\rho_k\rho_k^{T}} + (\boldsymbol{Q_{k-1}^{-\frac{1}{2}}})^{\mathrm{T}}\boldsymbol{\rho_k^{\mathrm{T}}}\right]^{-1}\boldsymbol{\Gamma^{\mathrm{T}}_{k-1}\Phi^{-\mathrm{T}}_{k/(k-1)}\xi_{k-1}}\right\} \tag{14}$$

In the equation, $\boldsymbol{\rho_k^{\mathrm{T}}}$ is obtained by performing QR decomposition on $\begin{bmatrix} \boldsymbol{\xi^{\mathrm{T}}_{k-1}\Phi^{-1}_{k/(k-1)}\Gamma_{k-1}} \\ \boldsymbol{Q_{k-1}^{-\frac{1}{2}}} \end{bmatrix}$.

The measurement update algorithm for the Square-Root Information Kalman Filter can be derived from the equation $\mathbb{I}_{\boldsymbol{k}} = \mathbb{I}_{\boldsymbol{k/(k-1)}} + \boldsymbol{H_k^{\mathrm{T}}R_k^{-1}H_k}$. Performing QR decomposition on $\begin{bmatrix} \boldsymbol{\xi^{\mathrm{T}}_{k/(k-1)}} \\ \boldsymbol{R_k^{-\frac{1}{2}}H_k} \end{bmatrix}$ yields $\boldsymbol{\xi_k^{\mathrm{T}}}$.

In the Square-Root Information Kalman Filter, the initial state estimation mean square error matrix can be set to infinity, corresponding to the information matrix being a zero matrix. Consequently, the initial square-root matrix $\boldsymbol{\xi_0}$ can also be set to the zero matrix, indicating a lack of initial information about the state.

5. Simulation Analysis

To verify the effectiveness of the Square-Root Information Kalman Filter in the SINS/GNSS integrated navigation system, a set of experimental data, including approximately 15 minutes of IMU and satellite receiver data, was selected for MATLAB simulation.

The IMU data includes timestamps, three-axis gyroscope measurements, and three-axis accelerometer measurements. The satellite receiver data includes timestamps, pseudorandom noise codes, ionosphere-free pseudorange linear combinations, tropospheric delay, ionospheric delay, relativistic corrections, satellite clock bias and drift, satellite position and velocity in the Earth-Centered Earth-Fixed (ECEF) frame, elevation angle, azimuth angle, and user range error. Satellite positioning systems employ the pseudorange-based single-point positioning method, which utilizes ionosphere-corrected pseudorange measurements and satellite clock bias corrections. By applying the least squares method, the three-dimensional position of the receiver is computed. Additionally, the residuals from the single-point positioning are used to evaluate the accuracy of the solution, enabling rapid and effective real-time positioning.

The system initial state is configured as follows: the initial attitude uncertainty is set to 20 °, the initial velocity uncertainty is set to 0.1 m/s, and the initial position uncertainty is set to 10 m. The initial accelerometer bias uncertainty of the IMU is set to 10,000 μm/s², and the initial gyroscope bias uncertainty of the IMU is set to 10 °/h. The initial clock bias is set to 10 m, and the initial clock drift is set to 0.1 m/s. The experimental parameters are configured as shown in Table 1 and Table 2.

Table 1. IMU Module Parameter Configuration

Parameter Names	Value	Unit
Gyroscope Noise Power Spectral Density	0.01	$(°/h)^2$/Hz
Accelerometer Noise Power Spectral Density	0.1	$(\mu g)^2$/Hz
Gyroscope Bias Random Walk Power Spectral Density	4.0×10^{-11}	rad^2/s^3
Accelerometer Bias Random Walk Power Spectral Density	1×10^{-5}	m^2/s^5

Table 2. GNSS Receiver Parameter Configuration

Parameter Names	Value	Unit
Observation Time Interval	1	s
Number of Satellites	30	/
Mask Angle	10	°
Receiver Clock Frequency Drift Power Spectral Density	1	m^2/s^3
Receiver Clock Phase Drift Power Spectral Density	1	m^2/s
Pseudorange Measurement Noise Standard Deviation	2.5	m
Pseudorange Rate Measurement Noise Standard Deviation	0.1	m/s

The system simulation error results of the square-root information extended Kalman filter algorithm are shown in Figure 2.

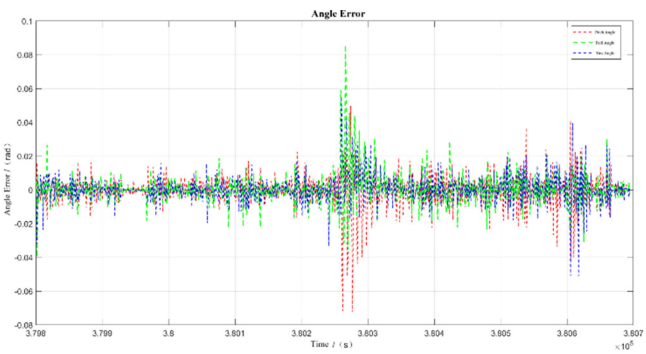

(a) Simulation Angle Error Plot of Tightly-Coupled Navigation System under Square-Root Information Kalman Filter

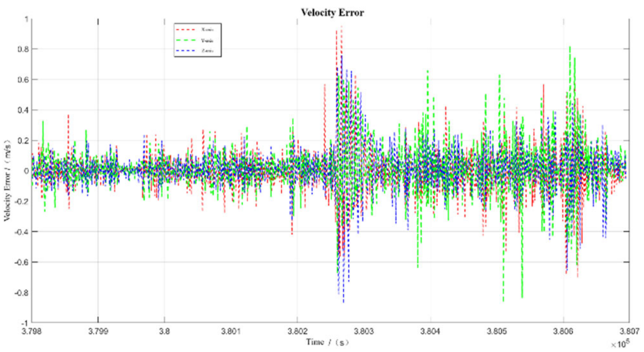

(b) Simulation Velocity Error Plot of Tightly-Coupled Navigation System under Square-Root Information Kalman Filter

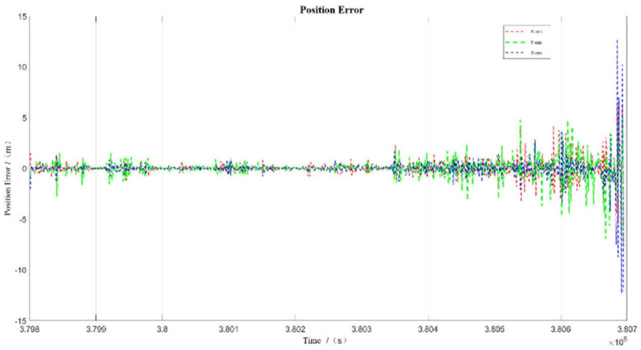

(c) Simulation Position Error Plot of Tightly-Coupled Navigation System under Square-Root Information Kalman Filter

Figure 2. Simulation Error Plots of the Tightly-Coupled Navigation System under Square-Root Information Kalman Filter

From the angle error plot, it can be observed that the angle errors of the system in all three directions are generally within the range of ±0.8 rad. Similarly, the velocity errors in all three directions are within the range of ±1 m/s. Nevertheless, the position error plot reveals that the Z-direction error surpasses ±10 meters. This can be addressed by integrating supplementary sensors, such as altimeters or barometers, to enhance altitude accuracy. Meanwhile, the errors in the X and Y directions are maintained within ±5 meters, well within the permissible limits of the navigation system.

The system calculations indicate that the standard deviations of the pitch, roll, and heading angle errors for the square-root information extended Kalman filter algorithm in the tightly-coupled navigation system simulation are 0.0093 rad, 0.0091 rad, and 0.0082 rad, respectively. Furthermore, the standard deviations of the velocity errors in the X, Y, and Z directions are 0.1536 m/s, 0.1592 m/s, and 0.1435 m/s, respectively, while the standard deviations of the position errors in the X, Y, and Z directions are 0.8569 m, 0.9711 m, and 1.0618 m, respectively. The navigation accuracy achieved by the square-root information extended Kalman filter algorithm falls within the acceptable range. The use of the square root of the information matrix for filter propagation enhances computational efficiency and ensures numerical stability.

The simulation results validate that the tightly-coupled navigation system employing the square-root information extended Kalman filter algorithm delivers superior estimation accuracy and reduced mean square error in nonlinear environments, highlighting its significant potential for nonlinear system applications. Consequently, integrating square-root information filtering into tightly-coupled navigation systems maximizes its strengths in managing nonlinearities, thereby boosting the system's capability to adapt to dynamic variations.

6. Conclusion

This paper thoroughly investigates the integrated navigation approach of the SINS/GNSS tightly-coupled navigation system and introduces the square-root information Kalman filter algorithm to enhance the system's accuracy and reliability. In summary, the proposed SINS/GNSS tightly-coupled navigation system based on the square-root information Kalman filter algorithm demonstrates significant advantages in improving navigation accuracy, suppressing error divergence, and enhancing anti-interference capabilities, highlighting its important theoretical and practical application value.

References

[1] Yang, S., Han, Y. K., & Jia, S. (2025). Application of GNSS/INS integrated navigation in flight approach and landing. Aeronautical Computing Technique, 55(1), 114-118.

[2] Zhou, Y., Wang, H., & Wang, J. (2025). GNSS/INS integrated positioning method in urban occlusion and multipath environments. Journal of Navigation and Positioning, 13(1), 113-118.

[3] Sun, S. G., Xu, Y. Z., & Wang, H. L. (2025). Research on INS/GNSS tightly coupled positioning algorithm for UAVs in GNSS-denied environments. Internet of Things Technologies, 15(1), 44-48.

[4] Sun, J. R., Meng, F. C., & Wang, D. Y. (2023). Code phase fault diagnosis and reconstruction algorithm for SINS/GNSS deeply integrated navigation. Journal of Chinese Inertial Technology, 31(6), 563-568.

[5] Cao, C. Y. (2023). Research on GPS/INS integrated navigation information fusion based on broad learning method (Doctoral dissertation, Dalian Maritime University).

[6] Jeong, K. Y., Park, D. Y., Kim, S. M., et al. (2021). Design of a compact GPS/MEMS IMU integrated navigation receiver module for high dynamic environment. The Korean Navigation Institute, 25(1).

[7] Chang, G., Xu, J., Li, A., et al. (2010). Error analysis and simulation of the dual-axis rotation-dwell autocompensating strapdown inertial navigation system. IEEE.

[8] Wang, N., & Liu, F. M. (2024). Application of adaptive fading memory square root mixed-order cubature particle filter based on constrained optimization in inertial/satellite integrated navigation. Journal of Jilin University (Engineering and Technology Edition), 54(12), 3660-3672.

[9] Tu, K. P., & Feng, S. J. (2023). A tightly coupled BDS/INS filtering method based on sequential processing. Optics & Optoelectronic Technology, 21(4), 130-137.

[10] Christophersen, H. B., Pickell, R. W., Neidhoefer, J. C., et al. (2006). A compact guidance, navigation, and control system for unmanned aerial vehicles. Journal of Aerospace Computing, Information, and Communication, 3(5).

[11] Wang, J. S., & Wang, X. L. (2013). Performance simulation analysis of SINS/GPS tightly coupled and loosely coupled navigation systems. Aero Weaponry, (2), 14-19.

[12] Yildiz, R., Barut, M., & Demir, R. (2020). Extended Kalman filter based estimations for improving speed-sensored control performance of induction motors. IET Electric Power Applications, 14(12), 2471-2479.

[13] Wang, T., Chen, Q., & Gao, P. (2024). Information filtering algorithm for maneuvering target tracking based on unbiased measurement conversion. Journal of Ordnance Equipment Engineering, 45(11), 19-24.

[14] Gao, Y. D., Zheng, N. S., Zhang, Y. S., et al. (2024). Phase unwrapping method based on phase quality fusion estimation and information filtering. Acta Geodaetica et Cartographica Sinica, 53(10), 1910-1919.